Non-Markovian effects on the dynamics of bubble growth in hot asymmetric nuclear matter

V. M. Kolomietz,[1,2] A. I. Sanzhur,[1] and S. Shlomo[2]
[1]*Institute for Nuclear Research, Kiev 03680, Ukraine*
[2]*Cyclotron Institute, Texas A&M University, College Station, Texas 77843, USA*
(Received 28 February 2003; published 30 July 2003)

We study the conditions for the generation and the dynamical evolution of embryonic overcritical vapor bubbles in an overheated asymmetric nuclear matter. We show that the Fermi-surface distortion and memory effects significantly hinder the growth of the bubbles. Moreover, the growth of the bubble is accompanied by characteristic oscillations of its radius R. The characteristic energy E, the damping parameter Γ, and the instability growth rate parameter ζ, depend on the relaxation time τ. The characteristic oscillations disappear in the short relaxation time limit $\tau \to 0$. Our approach ignores the fluctuations of the particle numbers in the bubble region and the finite diffuse layer of the bubble. The minimum size of the critical radius R^* for which our approach applies is determined by the condition $a/R^* \ll 1$, where $a = 0.5$–1 fm is the temperature-dependent surface thickness of the bubble.

DOI: 10.1103/PhysRevC.68.014614 PACS number(s): 21.65.+f, 24.10.Pa

I. INTRODUCTION

The boiling of a liquid is an example of a phase transition of the first order. The necessary condition for the boiling is the equilibrium between the liquid and the saturated vapor phases. Assuming a fixed external pressure P_0 and a plane surface for the separation of the liquid-vapor phases, the equilibrium conditions for the thermodynamical boiling point read [1]

$$P^{\mathrm{liq}}(T,\rho) = P^{\mathrm{vap}}(T,\rho) = P_0, \quad \mu^{\mathrm{liq}}(T,\rho) = \mu^{\mathrm{vap}}(T,\rho), \tag{1}$$

where P, μ, ρ and T are the pressure, chemical potential, particle density, and temperature, respectively. Here and in the following, the indices ''liq'' and ''vap'' denote the liquid and vapor phases, respectively. However, the conditions of Eq. (1) are not sufficient for the occurrence of the boiling process (cavitation). The boiling, as a process, also means the generation and the growth of the vapor phase (vapor bubbles) inside the liquid phase as a result of the heterophase fluctuations. In fact, the boiling can only start in a metastable phase (overheated or extended liquid). The formation of embryonic bubbles due to the quantum and statistical fluctuations was studied earlier in Refs. [2–4]. The spontaneous occurrence of embryonic bubbles caused by the single-particle fluctuations in hot nuclear matter was considered in Ref. [5]. We also point out that the process of the generation of vapor bubbles in the nuclear interior is interesting by itself because the expansion of a bubble means a breakdown of the nuclear liquid, i.e., the multifragmentation of the nucleus [6,7].

The process of boiling is usually considered for a given value of the pressure P_0. If at the pressure P_0 the equilibrium conditions (1) are satisfied for a certain value T_0 of the temperature, the generation of the critical vapor bubbles of radius R^*, which are in a thermodynamical equilibrium with the liquid, will start at a higher temperature T. The critical radius R^* depends on the overheating temperature $\delta T = T - T_0$ [8]. For a small embryonic bubble, the dynamical evolution of the bubble is influenced significantly by the fluctuation of the particle number in the bubble region. This effect was considered in Refs. [9,10] including a random force in the macroscopic equation of motion for the bubble radius. However, the macroscopic equation of motion used in Refs. [9,10] and earlier in Ref. [3] does not account for the effects of the Fermi-surface distortion on the transport coefficients. The purpose of this work is to study the features of the dynamical evolution of the bubble in the nuclear Fermi liquid, taking into account the influence of the Fermi motion of nucleons in the surrounding Fermi liquid on the bubble dynamics. We will consider the dynamical evolution of large enough overcritical bubbles ($R > R^*$) and neglect the single-particle fluctuations. Note that the number particle fluctuations play a significant role if the bubble radius is comparable with the average interparticle distance [9].

Our numerical analysis was carried out for the saturation temperature $T_0 = 6$ MeV, which corresponds to the plateau region in the nuclear caloric curve [11]. In this case, the lowest value of the critical radius R^* is about 4 fm, which seems to be too large to be applied directly to the problems of the heavy ion collisions. We point out, however, that the inclusion of the Coulomb forces, which is ignored in our nuclear matter consideration, decreases the value of R^* [2,3]. Unfortunately, the influence of the Coulomb forces on the formation of the vapor bubbles cannot be assessed for the case of infinite nuclear matter. Our consideration cannot be extended to very small values of R^*. It is self-evident that R^* cannot be smaller than the average distance between neighboring nucleons in the liquid phase. Moreover, for a small enough bubble the finite size effects, in particular the finite diffuse layer for the vapor density distribution inside the bubble, can be important [3]. In this respect, the minimum value of the radius R^*, for which our approach is applicable, is determined by the condition $a/R^* \ll 1$, where a is the surface thickness of the bubble. The parameter a can be extracted from the density profiles obtained in a temperature-dependent Hartree-Fock or Thomas-Fermi calculation, where $a = 0.5$–1 fm see Ref. [3] and references therein.

We will mainly focus on the dynamical effects related to the properties of the Fermi liquid. In particular, we will take into consideration the Fermi-surface distortion effects, memory effects (non-Markovian dynamics), and the relaxation processes. The dependence of the critical radius R^* on the overheating temperature δT for an asymmetric nuclear matter is considered in Sec. II. The equilibrium conditions for the heated nuclear matter and the saturated vapor are considered in Sec. III. The time development of the bubble instability in the thermodynamically metastable (overheated) nuclear matter is studied in Sec. IV. The summary is given in Sec. V.

II. CRITICAL BUBBLES IN OVERHEATED ASYMMETRIC NUCLEAR MATTER

Let us consider an asymmetric nuclear matter at a temperature T and an asymmetry parameter X, defined as $X=(\rho_n-\rho_p)/\rho$, where ρ_n and ρ_p are the neutron and proton densities, respectively. In the presence of both the liquid and the vapor (vapor bubble) phases, the equilibrium condition for the chemical potentials of neutrons, μ_n, and protons, μ_p, in the *absence of surface effects* (plane boundary surface) reads

$$\mu_q^{\rm liq}(P_0,T_0,X_{0,\rm liq})=\mu_q^{\rm vap}(P_0,T_0,X_{0,\rm vap}), \tag{2}$$

where q is the isospin index ($q=n$ for neutron and $q=p$ for proton). Let us fix the pressure $P_{\rm liq}=P_0$ and the asymmetry $X_{\rm liq}=X_{0,\rm liq}$ of the liquid phase. The two equilibrium conditions of Eq. (2) allow us to determine both the temperature T_0 and the asymmetry $X_{0,\rm vap}$ of saturated vapor in the case of plane geometry.

The boiling process takes place in the form of the generation of vapor bubbles which then grow to macroscopic dimensions. It thus becomes important to study the equilibrium of the bubble of radius R with respect to the surrounding liquid phase. A liquid which is overheated in the usual sense, i.e., with respect to a phase separated from it by a plane surface, can be underheated with respect to a vapor bubble of a finite radius R. We will extend equilibrium condition (2) in such a way that the liquid phase will remain in equilibrium with the vapor bubble with a given radius R, see also Ref. [8].

The thermodynamical potential of the whole system, consisting the liquid and the vapor bubble, is given by

$$\Phi=A_{\rm liq}\overline{\mu}_{\rm liq}(P_{\rm liq},T,X_{\rm liq})+A_{\rm vap}\overline{\mu}_{\rm vap}(P_{\rm vap},T,X_{\rm vap}), \tag{3}$$

where $A=N+Z$ is the number of nucleons (with N neutrons and Z protons) and $\overline{\mu}$ is the mean chemical potential, defined as

$$\overline{\mu}=\frac{1}{\rho}\sum_q \rho_q\mu_q=\frac{1+X}{2}\mu_n+\frac{1-X}{2}\mu_p. \tag{4}$$

We point out that due to the condition of mechanical equilibrium between the bubble and the surrounding liquid, the vapor pressure $P_{\rm vap}$ in the bubble must exceed the liquid one, $P_{\rm liq}$. Namely,

$$P_{\rm vap}=P_{\rm liq}+P_\sigma, \tag{5}$$

where P_σ is the capillary pressure,

$$P_\sigma=\frac{2\sigma}{R}, \tag{6}$$

and σ is the ordinary surface tension corresponding to $R=\infty$, i.e., we neglect the curvature corrections in σ. For fixed values of temperature T and pressure $P_{\rm liq}=P$ we derive the critical radius of bubble (R^*) from the condition of the thermodynamical equilibrium,

$$\delta\Phi/\delta A_{\rm vap}=0 \quad \text{at} \quad A_{\rm liq}+A_{\rm vap}=\text{const},$$

$$X_{\rm liq}A_{\rm liq}+X_{\rm vap}A_{\rm vap}=\text{const}. \tag{7}$$

Using Eqs. (3) and (7), we obtain

$$\mu_q^{\rm liq}(P,T,X_{\rm liq})-\mu_q^{\rm vap}\left(P+\frac{2\sigma}{R^*},T,X_{\rm vap}\right)=0. \tag{8}$$

We point out that in the limit of plane geometry, at $R^*\to\infty$, Eq. (8) is reduced to the standard condition of Eq. (2).

Differentiating both sides of Eq. (8) at fixed $X_{\rm liq}$ and T and using the relations

$$\left(\frac{\partial\overline{\mu}}{\partial P}\right)_{X,T}=\frac{1}{\rho}, \quad \left(\frac{\partial\overline{\mu}}{\partial X}\right)_{P,T}=\frac{\mu_n-\mu_p}{2},$$

we obtain (see also Ref. [8])

$$\left[\frac{1}{\rho_{\rm liq}(P,T,X_{\rm liq})}+2\Delta X\frac{\partial}{\partial X_{\rm liq}}\left(\frac{1}{\rho_{\rm liq}(P,T,X_{\rm liq})}\right)_{P,T}\right]dP$$

$$=\frac{dP+2\sigma d(1/R^*)}{\rho_{\rm vap}(P+2\sigma/R^*,T,X_{\rm vap})}, \tag{9}$$

where $\Delta X=(X_{\rm vap}-X_{\rm liq})/2$. Taking into account that $\rho_{\rm liq}\gg\rho_{\rm vap}$, one obtains from Eq. (9),

$$\delta P=P_0-P=\frac{2\sigma}{R^*}, \tag{10}$$

where P_0 is the pressure of a saturated vapor in the case of plane geometry at $R^*\to\infty$, see Eq. (2). As seen from Eq. (10), the undercompressed liquid with $P<P_0$ produces the cavitation in the liquid [the existence of the vapor bubble (critical bubble) in thermodynamical equilibrium with the surrounding liquid]. A comparison of Eqs. (10) and (5) leads to the following important relation $P_{\rm vap}=P_0$, i.e., the vapor pressure inside the critical bubble does not depend on its size [8].

The equilibrium condition (10) defines the bubble radius R^* in the undercompressed liquid as a function of the difference P_0-P for a given value of the temperature $T=T_0$, where T_0 is the boiling temperature in the case of plane geometry, see Eq. (2). We will now transform Eq. (10) to a different form, which describes the occurrence of cavitation in the overheated liquid for a given value of the external pressure P_0, where P_0 is the pressure for a saturated vapor in the plane geometry determined by Eq. (10). Let us establish the relation between the difference $\delta P=P_0-P$ and the overheating temperature $\delta T=T-T_0$. Both of them are due to the capillary pressure $P_\sigma^*=2\sigma/R^*$. We will consider a small variation of P, T, and $X_{\rm vap}$ in the equilibrium equation (8),

$$\mu_q^{\rm liq}(P_0-\delta P,T+\delta T,X_{0,\rm liq})=\mu_q^{\rm vap}(P_0,T+\delta T,X_{0,\rm vap}+\delta X_{\rm vap}). \tag{11}$$

We obtain from Eq. (11) the relation

$$\left[\frac{1}{\rho_{\rm liq}}+\Delta X\left(\frac{\partial\Delta\mu^{\rm liq}}{\partial P}\right)_{T,X}\right]_0\delta P=\left[\overline{s}^{\rm vap}-\overline{s}^{\rm liq}+\Delta X\left(\frac{\partial\Delta\mu^{\rm liq}}{\partial T}\right)_{P,X}\right]_0\delta T, \tag{12}$$

where $\Delta\mu^{\rm liq}=\mu_n^{\rm liq}-\mu_p^{\rm liq}$ and the subscript "0" means that all quantities are taken for the plane geometry as in Eq. (2). Here $\overline{s}$ is the entropy per particle given by

$$\overline{s}^{\rm vap}=\frac{S^{\rm vap}}{A_{\rm vap}}=-\left(\frac{\partial\overline{\mu}^{\rm vap}}{\partial T}\right)_{P,X},\quad \overline{s}^{\rm liq}=\frac{S^{\rm liq}}{A_{\rm liq}}=-\left(\frac{\partial\overline{\mu}^{\rm liq}}{\partial T}\right)_{P,X},$$

where S is the entropy. In deriving Eq. (12), we have used the relation

$$\frac{1+X}{2}\left(\frac{\partial\mu_n}{\partial X}\right)_{P,T}+\frac{1-X}{2}\left(\frac{\partial\mu_p}{\partial X}\right)_{P,T}=0.$$

Let us introduce the latent heat of evaporation

$$\overline{\phi}=\left[\frac{\overline{s}^{\rm vap}-\overline{s}^{\rm liq}+\Delta X(\partial\Delta\mu^{\rm liq}/\partial T)_{P,X}}{\rho_{\rm vap}/\rho_{\rm liq}+\rho_{\rm vap}\Delta X(\partial\Delta\mu^{\rm liq}/\partial P)_{T,X}}\right]_0 T_0. \tag{13}$$

Using Eqs. (10), (12), and (13), we obtain the critical radius of the overheated bubble as

$$R^*=\frac{2\sigma T_0}{\rho_{\rm vap}\overline{\phi}(T-T_0)}. \tag{14}$$

We point out that, in general, the surface tension depends on the temperature and the asymmetry parameter, namely, $\sigma=\sigma(T,X_{\rm liq})$.

Let us consider the change of the free energy of the liquid due to the formation of a bubble of an arbitrary radius R (i.e., not necessary stable with $R=R^*$). At fixed P, T, and X, it is given by the change of the corresponding thermodynamical potential,

$$\Delta\Phi=\Phi-\Phi_0, \tag{15}$$

where $\Phi_0=\overline{\mu}^{\rm liq}(A_{\rm liq}+A_{\rm vap})$ corresponds to the absence of the bubble. Taking into account that the surface free energy of the bubble is given by $4\pi R^2\sigma$, we obtain from Eq. (15),

$$\Delta\Phi=\overline{\mu}^{\rm liq}A_{\rm liq}+\overline{\mu}^{\rm vap}A_{\rm vap}+4\pi R^2\sigma-\overline{\mu}^{\rm liq}(A_{\rm liq}+A_{\rm vap})=(\overline{\mu}^{\rm vap}-\overline{\mu}^{\rm liq})\frac{4\pi}{3}R^3\rho_{\rm vap}+4\pi R^2\sigma. \tag{16}$$

At fixed P, T, and $X_{\rm liq}$, both chemical potentials $\overline{\mu}^{\rm vap}$ and $\overline{\mu}^{\rm liq}$ are also fixed, and they are related to each other by the equilibrium condition (7). Using

$$\Phi=\overline{\mu}^{\rm liq}A_{\rm liq}+\overline{\mu}^{\rm vap}A_{\rm vap}+4\pi R^2\sigma \tag{17}$$

and Eqs. (15), (16), and (7), one obtains the well-known result [8]

$$\Delta\Phi\equiv\Delta\Phi(R)=4\pi\sigma\left(R^2-\frac{2R^3}{3R^*}\right). \tag{18}$$

We point out that we neglect in our consideration the Coulomb forces because the Coulomb energy contribution to $\Delta\Phi$ is a rapidly decreasing function of the bubble size [2,9], and we will restrict ourselves by the bubble growth regime at $R>R^*$.

III. EQUATION OF STATE AND SURFACE OF EQUILIBRIUM WITHIN THE MEAN FIELD APPROXIMATION

To evaluate both the equilibrium vapor density $\rho_{\rm vap}$ and the latent heat of evaporation $\overline{\phi}$ in Eq. (14), we will follow the temperature-dependent Thomas-Fermi approximation using the Skyrme-type force as the effective nucleon-nucleon interaction. The free energy density $\mathcal{F}$ is given by [12,13]

$$\mathcal{F}=T\sum_q\left\{\mathcal{A}_q^*\left[J_{3/2}(\eta_q)-\frac{5}{3}J_{3/2}(\eta_q)\right]+\eta_q\rho_q\right\}+\frac{1}{2}t_0[(1+x_0/2)\rho^2-(x_0+1/2)(\rho_n^2+\rho_p^2)]+\frac{1}{12}t_3\rho^\sigma[(1+x_3/2)\rho^2-(x_3+1/2)(\rho_n^2+\rho_p^2)], \tag{19}$$

where x_i, t_i, and σ are the Skyrme force parameters, q is the isospin index ($q=n$ for neutrons and $q=p$ for protons), ρ_q is the nucleon density, and $\rho=\rho_n+\rho_p$. The Fermi integral $J_\nu(\eta_q)=\int_0^\infty dz\, z^\nu/[1+\exp(z-\eta_q)]$ in Eq. (19) depends on the fugacity η_q. The value of η_q can be found from the condition

$$\rho_q = \mathcal{A}_q^* J_{1/2}(\eta_q). \tag{20}$$

Here, $\mathcal{A}_q^* = (1/2\pi^2)(2m_q^* T/\hbar^2)^{3/2}$ and m_q^* is the effective nucleon mass, given by

$$\frac{\hbar^2}{2m_q^*} = \frac{\hbar^2}{2\,m_q} + \frac{1}{4}[t_1(1+x_1/2) + t_2(1+x_2/2)]\rho + \frac{1}{4}[t_2(x_2+1/2) - t_1(x_1+1/2)]\rho_q . \tag{21}$$

Using Eq. (19), one can derive the pressure P (equation of state) and the chemical potentials μ_q. Namely,

$$P = \rho^2 \left(\frac{\partial}{\partial \rho} \frac{\mathcal{F}}{\rho} \right)_{T,X},$$

$$\mu_n = \left(\frac{\partial \mathcal{F}}{\partial \rho_n} \right)_{T,\rho_p}, \quad \mu_p = \left(\frac{\partial \mathcal{F}}{\partial \rho_p} \right)_{T,\rho_n}. \tag{22}$$

A numerical calculation of the pressure P of Eq. (22) with the free energy density $\mathcal{F}$ from Eq. (19) leads to the van der Waals–like isotherms $P = P(T,X,\rho)$, describing both the liquid and the vapor phases in equilibrium [14–17]. Equilibrium states of the two-component (neutrons and protons) liquid-vapor system are located on the three-dimensional surface in the (P,T,X) space [13]. The (P,T,X) surface of equilibrium can be evaluated using the Gibbs equilibrium conditions [1] [see also Eq. (1)]:

$$P_{\rm liq}(T,X,\rho) = P_{\rm vap}(T,X,\rho), \quad \mu_q^{\rm liq}(T,X,\rho) = \mu_q^{\rm vap}(T,X,\rho). \tag{23}$$

Solving Eqs. (23) for certain values of $X_{\rm liq}$ and $T = T_0$, one obtains the equilibrium chemical potentials $\mu_{p,n}^{\rm liq} = \mu_{p,n}^{\rm vap}$, the vapor asymmetry parameter $X_{\rm vap}$, and the vapor density $\rho_{\rm vap}$. Determining these quantities allows us to evaluate the latent heat of evaporation $\overline{\phi}$, Eq. (13), and the radius R^* of the critical bubble, Eq. (14). Figure 1 shows the dependence of the critical radius R^* on the overheating temperature $\delta T = T - T_0$ for different values of the asymmetry parameter $X_{\rm liq}$ and a fixed boiling temperature $T_0 = 6$ MeV. The numerical calculations were performed using the SkM parameters x_i, t_i, and σ for the Skyrme force in Eq. (19) (see Ref. [13] for more details), and the surface tension coefficient σ is given by [18]

$$\sigma = 1.1 \left(\frac{T_C^2 - T^2}{T_C^2 + T^2} \right)^{5/4} \ \text{MeV}, \tag{24}$$

where $T_C = 14.6$ MeV is the critical temperature for infinite nuclear Fermi liquid, associated with the SkM interaction [13]. Figure 2 gives an illustration of the dependence of the overheating temperature δT on the change of the pressure (δP) in the undercompressed liquid obtained from the equilibrium equation (11). In the case of small variations δT and δP, the results shown in Fig. 2 agrees with those obtained from Eq. (12). The dependence of the overheating temperature δT on the asymmetry parameter $X_{\rm liq}$ is shown in Fig. 3. The increase of δT with $X_{\rm liq}$, seen in Fig. 3, is due to the fact that the increase of the temperature in an asymmetric nuclear matter leads to an increase of the value of the critical asymmetry parameter $X_{\rm liq}^{\rm crit}$ for the liquid-gas phase transition, see Ref. [13].

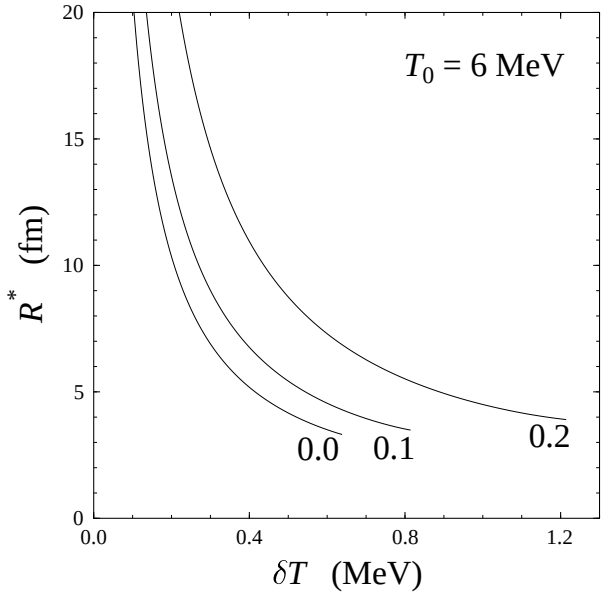

FIG. 1. Dependence of the critical radius R^* on the overheating temperature $\delta T = T - T_0$ for different values of the asymmetry parameter $X_{\rm liq} = 0$, 0.1, and 0.2 and fixed boiling temperature $T_0 = 6$ MeV. The numerical calculations were performed for the SkM force.

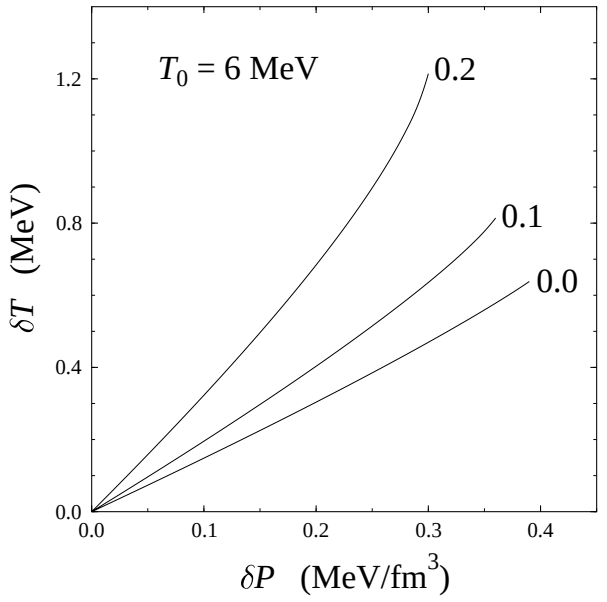

FIG. 2. Dependence of the overheating temperature δT on the pressure excess δP [see Eqs. (11) and (12)] for the values of the asymmetry parameter $X_{\rm liq} = 0$, 0.1, and 0.2 and a fixed boiling temperature $T_0 = 6$ MeV. The values of the asymmetry parameter $X_{\rm liq}$ are shown near the curves.

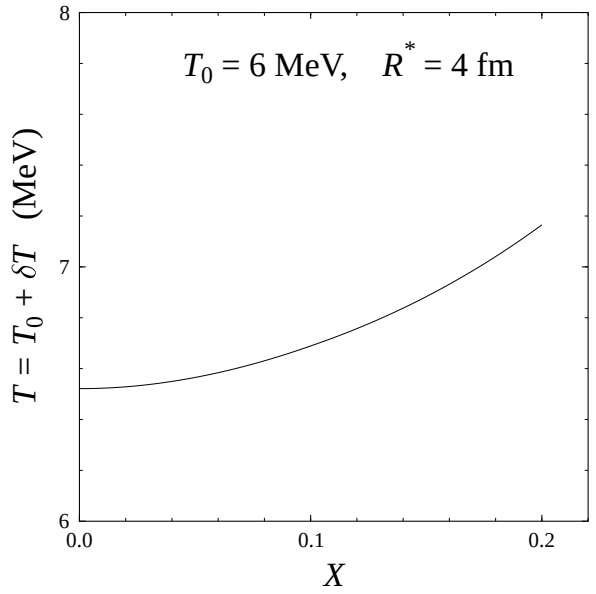

FIG. 3. Dependence of the overheating temperature δT on the asymmetry parameter $X_{\rm liq}$ for a fixed boiling temperature $T_0 = 6$ MeV and critical radius $R^* = 4$ fm.

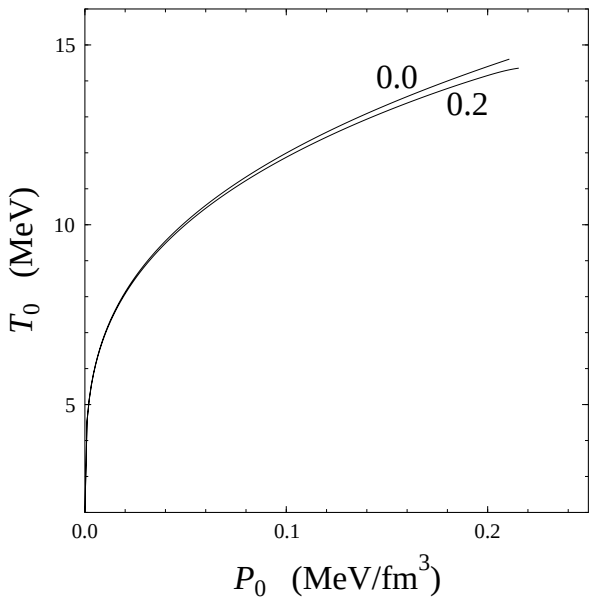

FIG. 4. Dependence of the boiling temperature T_0 on the equilibrium liquid-vapor pressure P_0 for the isobaric boiling of the asymmetric nuclear matter (no surface effects) for the values of the asymmetry parameter $X_{\rm liq} = 0$, 0.1, and 0.2.

The definition of the latent heat of evaporation $\overline{\phi}$ implies a fixed value of the boiling pressure P_0, see Eq. (13). The numerical estimate of the boiling pressure P_0 and the corresponding boiling temperature T_0 can be obtained by studying the caloric curve for the case of isobaric heating. Let us consider the temperature dependence of the excitation energy per particle, E^*A, which is given by

$$\frac{E^*}{A} = \frac{\lambda_{\rm liq}\mathcal{E}_{\rm liq}(\rho_{\rm liq}, X_{\rm liq}, T) + \lambda_{\rm vap}\mathcal{E}_{\rm vap}(\rho_{\rm vap}, X_{\rm vap}, T)}{\lambda_{\rm liq}\rho_{\rm liq} + \lambda_{\rm vap}\rho_{\rm vap}} - \left(\frac{\mathcal{E}_{\rm liq}(\rho_{\rm liq}, X_{\rm liq}, T)}{\rho_{\rm liq}}\right)_{T=0}, \tag{25}$$

where $\mathcal{E} = \mathcal{F} + T\mathcal{S}$ is the energy density and $\mathcal{S}$ is the entropy density,

$$\mathcal{S} = \sum_q \left(\frac{5}{3}\mathcal{A}_q^* J_{3/2}(\eta_q) - \eta_q \rho_q\right). \tag{26}$$

The volume fractions $\lambda_{\rm liq}$ and $\lambda_{\rm vap}$ of the liquid and vapor phases in Eq. (25) are defined by $\lambda_{\rm liq} = V_{\rm liq}/V$ and $\lambda_{\rm vap} = V_{\rm vap}/V$, where $V_{\rm liq}$ and $V_{\rm vap}$ are the volumes of the liquid and vapor phases, respectively, and $V = V_{\rm liq} + V_{\rm vap}$. Numerical calculations show [13] that the low temperature dependence of the excitation energy E^*A corresponds to the heating of the degenerate Fermi liquid with $E^*A \sim T^2$. At high temperatures, the excitation energy E^*A dependence on T is the same as that of the classical Boltzmann's gas with $E^*A = (3/2)T$. The caloric curve $T(E^*/A)$ is a continuous function and has a plateau region for two-phase coexistence. The plateau region is achieved at a certain temperature T_0, which depends significantly on the pressure P_0. The temperature T_0 can be identified as the boiling temperature (first-order phase transition temperature). In Fig. 4, the dependence of the boiling temperature T_0 on the "external" pressure P_0 is shown for different values of the asymmetry parameter $X_{\rm liq}$. Experimental observations show a nearly flat (plateau) caloric curve with a temperature of about 7 MeV [11]. If one could assume the process of isobaric heating for the description of the experimental data, the order of magnitude of the pressure P_0 should be $P_0 \approx 10^{-2}$ MeV/fm^3 for this process. Below we will use this value of P_0 as the external pressure for the boiling in an overheated Fermi liquid.

IV. HETEROPHASE FLUCTUATIONS AND BOILING

Let us consider the dynamical evolution of overcritical bubbles in an overheated nuclear matter. As noted earlier, the bubble with the critical size $R = R^*$ exists in a thermodynamic equilibrium with the liquid. The distribution of such bubbles with respect to their size is given by Gibbs's formula [1,8]

$$W = \text{const}(e^{-\Delta\Phi(R^*)/T}), \tag{27}$$

where the potential $\Delta\Phi(R^*)$ is given by [see Eq. (18)]

$$\Delta\Phi(R^*) = \frac{4}{3}\pi\sigma {R^*}^2. \tag{28}$$

We now consider the dynamics of the bubble with an arbitrary overcritical size $R > R^*$. In Fig. 5 we have plotted the thermodynamical potential $\Delta\Phi(R)$ as a function of the bubble radius R [see Eq. (18)] for the overheated liquid with $T > T_0$ (solid line) and for a temperature T below the boiling temperature T_0 (dashed line). The position of the maximum of the curve $\Delta\Phi(R)$ is located at $R = R^*$, and it is shifted to

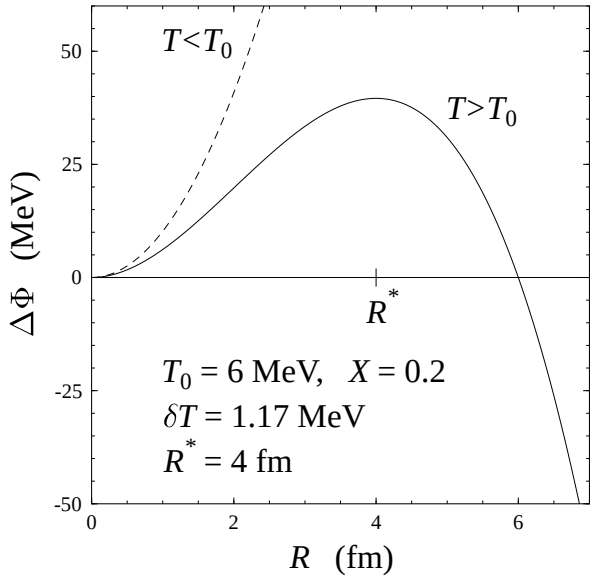

FIG. 5. Dependence of the thermodynamical potential $\Delta\Phi$ [see Eq. (18)] of metastable liquid on the radius of the bubble. The solid line is for the overheated liquid with $T>T_0$ and the dashed line is for $T<T_0$.

the left with the increase of the overheating temperature $\delta T = T - T_0$, because of Eq. (14). As one can see from Fig. 5, the point $R=R^*$ is the critical point for the metastable phase in the following sense: to start the boiling process, i.e., to start the process of increasing the size of the bubbles, the system must pass through the barrier $\Delta\Phi(R)$ to reach the region of $R>R^*$.

To describe the development of instability of the bubble with a nonequilibrium size $R>R^*$, one needs to know the equation of motion for the time dependence of $R=R(t)$. To obtain the macroscopic equation of motion for the bubble radius $R(t)$, we will start from the collisional kinetic equation for the phase-space distribution function $f\equiv f(\mathbf{r},\mathbf{p};t)$ in the following form:

$$\frac{\partial}{\partial t}f+\frac{\mathbf{p}}{m}\cdot\boldsymbol{\nabla}_r f-\boldsymbol{\nabla}_r U\cdot\boldsymbol{\nabla}_p f=-\frac{\delta f_{\{l\geqslant 2\}}}{\tau}, \tag{29}$$

where $U\equiv U(\mathbf{r},\mathbf{p};t)$ is the self-consistent mean field, $-\delta f_{\{l\geqslant 2\}}/\tau$ is the collision integral, τ is the relaxation time, and l is the multipolarity of the Fermi-surface distortion. The notation $\delta f_{\{l\geqslant 2\}}$ in Eq. (29) means that the collision integral does not contain the components with $l=0$ and $l=1$ for the distorted distribution function δf in momentum space because of the conservation of the number of particles and of the total momentum. Note that Eq. (29) can be easily extended by including the random forces in the right hand side of the equation, see Ref. [19]. Therefore, the fluctuation of the particle number in the bubble region can be taken into consideration in our approach in a way similar to the approach of Ref. [9].

The momentum distribution is distorted during the dynamical evolution of the bubble, and the distribution function takes the form

$$f(\mathbf{r},\mathbf{p};t)=f_{\rm sph}(\mathbf{r},\mathbf{p};t)+\sum_{l\geqslant 1}\delta f_l(\mathbf{r},\mathbf{p};t), \tag{30}$$

where $f_{\rm sph}(\mathbf{r},\mathbf{p};t)$ describes the spherical distribution in momentum space. We point out that the time-dependent Thomas-Fermi (TDTF) approximation is obtained from Eq. (29) if one takes the distribution function $f(\mathbf{r},\mathbf{p};t)$ in the following restricted form $f_{\rm TF}(\mathbf{r},\mathbf{p};t)=f_{\rm sph}(\mathbf{r},\mathbf{p};t)+\delta f_{l=1}(\mathbf{r},\mathbf{p};t)$, instead of Eq. (30), see Ref. [20]. Below we will extend the TDTF approximation taking into account the dynamic Fermi-surface distortion up to multipolarity $l=2$. We will also assume that the collective motion is accompanied by a small deviation of the momentum distribution from the spherical symmetry, i.e., even in the case of large amplitude motion the main contribution to the distribution function $f(\mathbf{r},\mathbf{p};t)$ is given by the Thomas-Fermi term $f_{\rm TF}(\mathbf{r},\mathbf{p};t)$, and the additional term $\delta f_{l=2}(\mathbf{r},\mathbf{p};t)$ provides only a small correction. The lowest orders $l=0$ and 1 (which are not necessarily small) of the Fermi-surface distortion do not contribute to the collision integral in Eq. (29) because of the particle number and momentum conservation in an interparticle collision.

Evaluating the first three moments of Eq. (29) in $\mathbf{p}$ space, we can derive a closed set of equations for the following moments of the distribution function, namely, the local particle density ρ, the velocity field u_ν, and the pressure tensor $P_{\nu\mu}$, in the form (for details, see Refs. [20,21])

$$\frac{\partial}{\partial t}\rho=-\nabla_\nu(\rho u_\nu), \tag{31}$$

$$m\rho\frac{\partial}{\partial t}u_\nu+m\rho(u_\mu\nabla_\mu)u_\nu+\nabla_\nu\mathcal{P}+\rho\nabla_\nu\frac{\delta\epsilon_{\rm pot}}{\delta\rho}=-\nabla_\mu P'_{\nu\mu}, \tag{32}$$

$$\frac{\partial}{\partial t}P'_{\nu\mu}+\mathcal{P}\frac{\partial}{\partial t}\Lambda_{\nu\mu}=-\frac{1}{\tau}P'_{\nu\mu}. \tag{33}$$

Here

$$\rho=\int\frac{d\mathbf{p}}{(2\pi\hbar)^3}f,\quad u_\nu=\frac{1}{\rho}\int\frac{d\mathbf{p}}{(2\pi\hbar)^3}\frac{p_\nu}{m}f, \tag{34}$$

and $\mathcal{P}\equiv\mathcal{P}(\mathbf{r},t)$ is the isotropic part of the pressure tensor,

$$\mathcal{P}(\mathbf{r},t)=\frac{1}{3m}\int\frac{d\mathbf{p}}{(2\pi\hbar)^3}p^2 f_{\rm sph}(\mathbf{r},\mathbf{p};t)=(2/3)\epsilon_{\rm kin}. \tag{35}$$

Here, $\epsilon_{\rm kin}\approx(3/5)\rho\epsilon_F$ is the internal kinetic energy and ϵ_F is the Fermi energy. The tensor $P'_{\nu\mu}=P'_{\nu\mu}(\mathbf{r},t)$ is the deviation of the pressure tensor from its isotropic part, $\mathcal{P}(\mathbf{r},t)$, due to the Fermi-surface distortion,

$$P'_{\nu\mu}(\mathbf{r},t)=\frac{1}{m}\int\frac{d\mathbf{p}}{(2\pi\hbar)^3}(p_\nu-mu_\nu)(p_\mu-mu_\mu)\delta f_{l=2}(\mathbf{r},\mathbf{p};t). \tag{36}$$

The potential energy density $\epsilon_{\rm pot}$ in Eq. (32) is related to the self-consistent mean field U as $U=\delta\epsilon_{\rm pot}/\delta\rho$, and the tensor $\Lambda_{\nu\mu}$ in Eq. (33) is given by

$$\Lambda_{\nu\mu}=\nabla_\nu\chi_\mu+\nabla_\mu\chi_\nu-\frac{2}{3}\delta_{\nu\mu}\nabla_\lambda\chi_\lambda, \tag{37}$$

where $\chi_\nu\equiv\chi_\nu(\mathbf{r},t)$ is the displacement field which is related to the velocity field by $u_\nu\equiv u_\nu(\mathbf{r},t)=\partial\chi_\nu(\mathbf{r},t)/\partial t$. From Eq. (33) we find the pressure tensor $P'_{\nu\mu}(\mathbf{r},t)$ in the form

$$P'_{\nu\mu}(\mathbf{r},t)=P'_{\nu\mu}(\mathbf{r},t_0)\exp\left(\frac{t_0-t}{\tau}\right)-\int_{t_0}^{t}dt'\exp\left(\frac{t'-t}{\tau}\right)\mathcal{P}(\mathbf{r},t')\frac{\partial}{\partial t'}\Lambda_{\nu\mu}(\mathbf{r},t'). \tag{38}$$

A solution of the continuity equation for the spherical bubble leads to the following displacement field χ in the surrounding liquid [3,22]:

$$\chi_\nu(r,t)=\frac{R^3}{3r^2}\frac{r_\nu}{r},\quad r\geqslant R. \tag{39}$$

Multiplying Eq. (32) by $\overline{\chi_\mu}=u_\mu/\dot{R}$ and integrating over $\mathbf{r}$, one obtains the following non-Markovian equation for the collective variable $R(t)$:

$$B\ddot{R}+\frac{1}{2}\frac{\partial B}{\partial R}\dot{R}^2+\int_{t_0}^{t}dt'\dot{R}(t')\exp\left(\frac{t'-t}{\tau}\right)\mathcal{K}(t,t')=-\frac{\partial E_{\rm pot}}{\partial R}. \tag{40}$$

The inertial parameter B in Eq. (40) can be derived from the definition of the collective kinetic energy $E_{\rm kin}$. Namely,

$$E_{\rm kin}=\frac{m}{2}\int d\mathbf{r}\rho u^2=\frac{1}{2}B\dot{R}^2.$$

Assuming $\rho_{\rm vap}\ll\rho_{\rm liq}\approx\rho=\rho_0\theta(r-R)$, we obtain [3]

$$B=4\pi mR^3\rho_0. \tag{41}$$

The collective potential energy $E_{\rm pot}(R)$ in Eq. (40) can be identified with the thermodynamical potential of Eq. (18). Namely,

$$E_{\rm pot}(R)=\Delta\Phi(R). \tag{42}$$

Finally, the memory kernel $\mathcal{K}(t,t')$ in Eq. (40) is given by

$$\mathcal{K}(t,t')=\int d\mathbf{r}\mathcal{P}(\mathbf{r},t')[\nabla_\nu\overline{\chi_\mu}(\mathbf{r},t)]\left[\nabla_\nu\chi_\mu(\mathbf{r},t')+\nabla_\mu\chi_\nu(\mathbf{r},t')-\frac{2}{3}\delta_{\nu\mu}\nabla_\lambda\chi_\lambda(\mathbf{r},t')\right]. \tag{43}$$

Using Eqs. (35), (39), and (43), we obtain

$$\mathcal{K}(t,t')=(32/5)\pi\rho_0\epsilon_F R(t). \tag{44}$$

We point out that the non-Markovian form of Eq. (40) is due to the effects of the Fermi-surface distortion. The memory integral in Eq. (40) provides both the friction and the conservative time-reversible force in Eq. (40). Also note that we neglect the quantum and statistical (single-particle) fluctuations in Eq. (40). The quantum fluctuations play an insignificant role for temperatures $T\gtrsim 1$ MeV [2,3]. The single-particle fluctuations can change the bubble dynamics, especially for R near the critical value R^*, see Ref. [9], if the bubble radius R is comparable with the average interparticle distances. Below we will apply Eq. (40) to the regions of T and R where the quantum and the single-particle fluctuations are negligible.

For a small amplitude motion near the top of the barrier (the starting path for the development of the instability), Eq. (40) is reduced for $\Delta R=R-R^*$ as

$$B^*\frac{\partial^2}{\partial t^2}\Delta R=-k\Delta R-\tilde{\kappa}\int_{t_0}^{t}dt'\exp\left(\frac{t'-t}{\tau}\right)\frac{\partial}{\partial t'}\Delta R(t'), \tag{45}$$

where

$$B^*=4\pi mR^{*3}\rho_0,\quad k=\partial^2\Delta\Phi(R)/\partial R^2|_{R=R^*}=-8\pi\sigma$$

$$\text{and}\quad \tilde{\kappa}=(32/5)\pi\rho_0\epsilon_F R^*.$$

We also point out that for two limiting cases of rare ($\tau\to 0$) and frequent ($\tau\to\infty$) collision regimes, Eq. (45) is reduced to the standard Newton's equation. For both limiting cases, we obtain from Eq. (45),

$$B^*\frac{\partial^2}{\partial t^2}\Delta R(t)=-k'\Delta R-\gamma\frac{\partial}{\partial t}\Delta R(t), \tag{46}$$

where $k'=k$ if $\tau\to 0$ and $k'=k+\tilde{\kappa}$ if $\tau\to\infty$. The friction coefficient γ in Eq. (46) will be derived and discussed below.

We will look for the solution to Eq. (45) in the form

$$\Delta R=\sum_{i=1}^{3}C_i\exp(\lambda_i t), \tag{47}$$

where the coefficients C_i are determined by the initial conditions. Differentiating Eq. (45) over time we find that the eigenvalues λ_i can be obtained as solutions to the following secular equation:

$$\left(\lambda^2+\frac{k}{B^*}\right)\left(\lambda+\frac{1}{\tau}\right)+\frac{\tilde{\kappa}}{B^*}\lambda=0, \tag{48}$$

where τ is the relaxation time. In the case of the zero-relaxation-time limit $\tau\to 0$, one obtains from Eq. (48) a non-damped motion with $\lambda=\pm\sqrt{|k|/B^*}$, i.e., the time evolution is derived by the static stiffness coefficients k. In the opposite case of rare collisions, $\tau\to\infty$, the solution to Eq. (48) leads to a motion with $\lambda=\pm i\sqrt{(-|k|+\tilde{\kappa})/B^*}$. In contrast to the

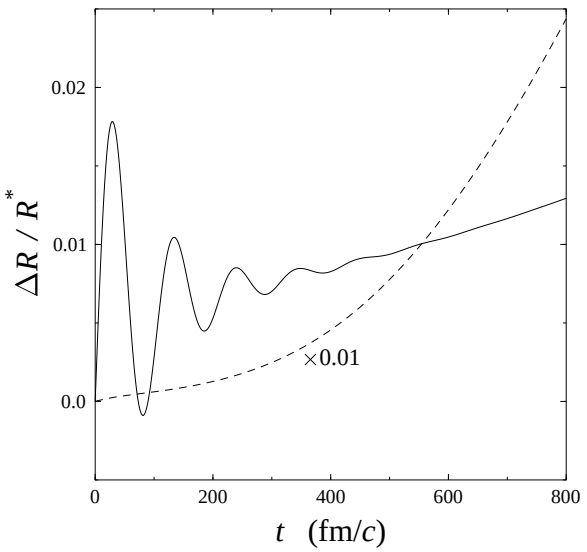

FIG. 6. Time variation of the bubble shape parameter R near the barrier point $R=R^*$ for various values of the relaxation time τ. The dashed and solid curves correspond to the values of $\tau=5$ fm/c and $\tau=50$ fm/c, respectively.

previous case, the additional contribution $\tilde{\kappa}$ appears at the stiffness coefficient $-|k|+\tilde{\kappa}$ because of the Fermi-surface distortion effect.

In a general case of arbitrary τ, solution (47) takes the form

$$\Delta R = C_\zeta e^{\zeta t} + A_\omega e^{-\Gamma t/2\hbar}\sin(Et/\hbar) + B_\omega e^{-\Gamma t/2\hbar}\cos(Et/\hbar). \tag{49}$$

We have evaluated numerically the value of ΔR from Eq. (45) using the secular equation (48) and the initial conditions

$$\Delta R(t_0)=0, \quad \frac{\partial}{\partial t}\Delta R(t)\big|_{t=t_0}=v_0, \quad \text{and}$$

$$\frac{\partial^2}{\partial t^2}\Delta R(t)\big|_{t=t_0}=0,$$

where v_0 is the initial velocity. In Fig. 6 we show the results for two values of the relaxation time, $\tau=5$ fm/c (dashed line) and $\tau=50$ fm/c (solid line). We have used $R^*=4$ fm, and the initial velocity v_0 was derived using the initial kinetic energy $E_{\mathrm{kin},0}=(1/2)B_f v_0^2=1$ MeV.

In the case of the very short relaxation time $\tau=5$ fm/c (frequent collision regime), the memory effects in Eq. (45) play only a minor role (Markovian regime), and the amplitude of motion is approximately an exponentially growing function, similar to the case of Newton motion from the barrier in the presence of the friction forces, see the dashed curve in Fig. 6. The friction coefficient γ was derived here from Eq. (45) at $\omega_F\tau \ll 1$, and it is given by $\gamma=\tilde{\kappa}\tau=\omega_F^2 B^*\tau \sim \tau$, where $\omega_F=\sqrt{\tilde{\kappa}/B^*}$ is the characteristic frequency for the eigenvibrations caused by the Fermi-surface distortion effect. We also point out that since Eq. (45) is only applicable for small amplitude ΔR, the dashed line in Fig. 6 was obtained using the exact solution of Eq. (40).

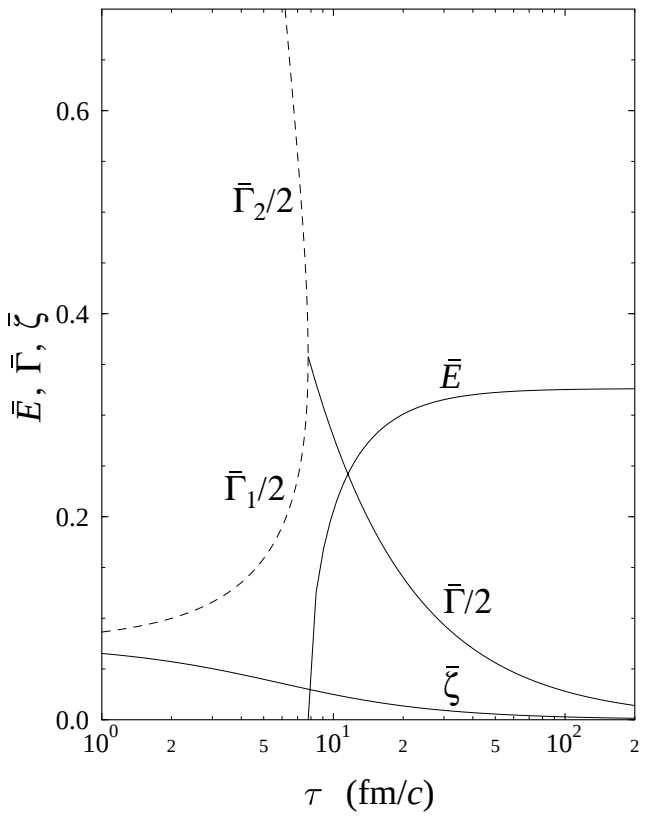

FIG. 7. Dependence upon relaxation time τ of the dimensionless values of the characteristic energy $\bar{E}=E/\epsilon_F$, width $\bar{\Gamma}=\Gamma/\epsilon_F$, and the instability growth rate parameter $\bar{\zeta}=\zeta/\epsilon_F$ for the case of Eq. (49) and for damping parameters $\bar{\Gamma}_1=\Gamma_1/\epsilon_F$ and $\bar{\Gamma}_2=\Gamma_2/\epsilon_F$ in the case of the solution given by Eq. (50).

At large enough relaxation time, the bubble growth depends essentially on the memory effects (non-Markovian regime). The solid line in Fig. 6 shows $\Delta R(t)$ obtained from Eq. (46) for $\tau=50$ fm/c. As can be seen from Fig. 6, the behavior of $\Delta R(t)$ is changed dramatically with the increase of the relaxation time. For the large relaxation time, a significant time delay in the increase of the bubble size arises due to the non-Markovian effects. Moreover, the bubble growth is accompanied by damped oscillations. These oscillations are due to the memory integral in Eq. (45). The characteristic frequency ω_R and the corresponding damping parameter ω_I can be derived from the imaginary and real parts of the complex conjugate roots of Eq. (48) as $\lambda=-\omega_I \pm i\omega_R$ with $\Gamma=2\hbar\omega_I$ and $E=\hbar\omega_R$.

In Fig. 7 we show the dependence of the instability growth rate parameter ζ [see Eq. (49)], the energy of eigenvibrations (E), and the damping parameter Γ on the relaxation time τ. For small enough values of the relaxation time, $\tau \lesssim 8$ fm/c, the function $\Delta R(t)$ does not oscillate with time and takes the following form [compare with Eq. (49) and see the dashed lines in Fig. 7]:

$$\Delta R = C_\zeta e^{\zeta t} + C_1 e^{-\Gamma_1 t/2\hbar} + C_2 e^{-\Gamma_2 t/2\hbar}. \tag{50}$$

We point out that the behavior of the friction coefficient γ in the above mentioned relaxation regimes is essentially different. In the rare collision regime $\omega_F\tau \gg 1$, the friction coefficient γ in the equation of motion (46) is obtained from Eq. (45) as $\gamma = B^*/\tau \sim 1/\tau$. This τ dependence of the friction coefficient, $\gamma \sim 1/\tau$, is caused by the dynamical Fermi-surface distortions [19], and it is opposite to the τ dependence of $\gamma \sim \tau$ in the short relaxation regime $\omega_F\tau \ll 1$ (see above). In general, one can use the following extrapolation form for the friction coefficient:

$$\gamma = \omega_F B^* \frac{\omega_F\tau}{1+(\omega_F\tau)^2}, \tag{51}$$

which provides the correct limit for γ in both $\tau \to 0$ and $\tau \to \infty$ cases.

We also point out that the presence of the characteristic oscillations of the bubble radius behind the barrier with $R > R^*$ can lead to the emission of γ quanta. The energy $E = \hbar\omega_R$ and the damping $\Gamma = 2\hbar\omega_I$ of this radiation depend both on the phase transition, T_0, and the overheating, δT, temperatures. This fact can be used for the determination of both temperatures T_0 and δT from the measurement of the characteristics E and Γ of the corresponding resonance line. For the uncharged nuclear matter, the energy E and the damping parameter Γ are given in Fig. 7. In the following step in the investigation of cavitation in nuclear liquid, we plan to take into account the finite size and the charge of the nucleus for both the liquid and the vapor phase.

V. SUMMARY

Using the temperature-dependent Thomas-Fermi approximation [13] and the Skyrme-type forces as the effective nucleon-nucleon interaction, we have solved equilibrium equations (23) and evaluated the dependence of the critical radius R^* of the embryonic bubble on the overheating temperature δT. We pointed out that the critical radius R^* increases with the asymmetry parameter $X_{\rm liq}$ of the liquid phase. This is mainly due to the increase of the boiling temperature T_0 with the decrease of the asymmetry parameter $X_{\rm liq}$, see Ref. [13].

The generation of the embryonic bubble of arbitrary radius R is subsidized by the variation of the free energy $\Delta\Phi(R)$, which is given by Eq. (18), see also Fig. 5. The maximum of $\Delta\Phi(R)$ is located at $R = R^*$, and its position is shifted to smaller values of R^* with an increase of the overheating temperature δT. The bubble radius R^* is the critical point for the metastable phase with respect to the boiling process. To start the boiling up (cavitation), i.e., to start the infinite growth in the size of the bubbles, the system must pass through the barrier of $\Delta\Phi(R)$ to reach the region of $R > R^*$.

We have studied the problem of the dynamical evolution of the overcritical bubble with the radius R behind the barrier at $R > R^*$. Starting from the collisional kinetic equation for the nuclear Fermi liquid, we have derived the non-Markovian equation of motion for the bubble radius $R(t)$ without restrictions on the amplitude of $\Delta R = R(t) - R^*$.

We have shown that the development of instability of the bubble near the barrier point $R = R^*$ is strongly influenced by the memory effects, if the relaxation time τ is large enough. In this case, an expansion of the bubble is accompanied by characteristic shape oscillations of the bubble radius (see Figs. 6 and 7), which depend on the parameter $\tilde{\kappa}$ of the memory kernel and on the relaxation time τ. Oscillations of the radius appear due to the elastic force induced by the memory integral. This elastic force acts against the adiabatic force $-k\Delta R$ [see Eq. (45)] and hinders the growth of the bubble radius. In contrast to the case of the Markovian motion, the delay in the boiling process is caused here by *both* the conservative elastic and the friction forces, and not by the friction force alone. We point out that the emission of γ quanta becomes possible due to the characteristic shape oscillations of the bubble size. This fact provides, in principle, the possibility for the measurement of the temperature of the first kind phase transition through the measurement of the energy and the damping of the corresponding resonances in the γ-quanta spectrum.

ACKNOWLEDGMENTS

This work was supported in part by the U.S. Department of Energy under Grant No. DOE-FG03-93ER40773. One of us (V.M.K.) thanks the Cyclotron Institute at Texas A&M University for the kind hospitality.

[1] L. D. Landau and E. M. Lifshitz, Statistical Physics (Pergamon, Oxford, 1958).
[2] A.H. Blin *et al.*, Phys. Lett. B **182**, 239 (1986).
[3] A.H. Blin, B. Hiller, H. Reinhardt, and P. Schuck, Nucl. Phys. **A484**, 295 (1988).
[4] H. Schulz, D.N. Voskresensky, and J.P. Bondorf, Phys. Lett. B **113**, 141 (1983).
[5] R. Donangelo, K. Sneppen, and J.P. Bondorf, Phys. Lett. B **219**, 165 (1989).
[6] C.J. Pethick and D.G. Ravenhall, Nucl. Phys. **A471**, 19c (1987).
[7] F.F. Abraham, Phys. Rep. **53**, 93 (1979).
[8] J. Frenkel, *Kinetic Theory of Liquids* (Clarendon, Oxford, 1946).
[9] J.P. Bondorf, R. Donangelo, and K. Sneppen, Phys. Lett. B **214**, 321 (1988).
[10] A.J. Santiago and K.C. Chung, Nuovo Cimento Soc. Ital. Fis., A **105**, 1729 (1992).
[11] J. Cibor *et al.*, Phys. Lett. B **473**, 29 (2000).
[12] M. Brack, C. Guet, and H.-B. Håkansson, Phys. Rep. **123**, 275 (1985).
[13] V.M. Kolomietz, A.I. Sanzhur, S. Shlomo, and S.A. Firin, Phys. Rev. C **64**, 024315 (2001).
[14] G. Sauer, H. Chandra, and U. Mosel, Nucl. Phys. **A264**, 221

(1976).
[15] J.M. Lattimer and D.G. Ravenhall, Astrophys. J. **223**, 314 (1978).
[16] D.Q. Lamb, J.M. Lattimer, C.J. Pethick, and D.G. Ravenhall, Nucl. Phys. **A360**, 459 (1981).
[17] J.M. Lattimer, C.J. Pethick, D.G. Ravenhall, and D.Q. Lamb, Nucl. Phys. **A432**, 646 (1985).
[18] D.G. Ravenhall, C.J. Pethick, and J.M. Lattimer, Nucl. Phys. **A407**, 571 (1983); D.G. Ravenhall, C.J. Pethick, and J.R. Wilson, Phys. Rev. Lett. **50**, 2066 (1983).
[19] D. Kiderlen, V.M. Kolomietz, and S. Shlomo, Nucl. Phys. **A608**, 32 (1996).
[20] V.M. Kolomietz and H.H.K. Tang, Phys. Scr. **24**, 915 (1981).
[21] V.M. Kolomietz, S.V. Radionov, and S. Shlomo, Phys. Rev. C **64**, 054302 (2001).
[22] H. Lamb, *Hydrodynamics* (Dover, New York, 1932).